[14]R. Marriott, Proc. Phys. Soc. 87, 407 (1966).
[15]A. V. Phelps, Phys. Rev. 99, 1307 (1955).
[16]S. C. Brown, Basic Data of Plasma Physics, 1966 (MIT Press, Cambridge, Mass., 1967), p. 57.
[17]*Ibid.*, p. 17.
[18]R. W. Huggins and J. H. Cahn, J. Appl. Phys. 38, 180 (1967).
[19]P. M. Banks, Ann. Geophys. 22, 577 (1966).
[20]A. N. Kaufman, in Plasma Physics in Theory and Application, edited by W. B. Kunkel (McGraw-Hill Book Company, New York, 1966), p. 113.
[21]D. J. Collins, R. Greif, and A. E. Bryson, Jr., Intern. J. Heat Mass Transfer 8, 1209 (1965).
[22]L. Spitzer, Jr., Physics of Fully Ionized Gases (Interscience Publishers, Inc., New York, 1962), p. 135
[23]M. A. Biondi and S. C. Brown, Phys. Rev. 75, 1700 (1949).

PHYSICAL REVIEW VOLUME 179, NUMBER 1 5 MARCH 1969

Spectroscopic Measurement of High-Frequency Electric Fields in a Plasma by Observation of Two-Quantum Transitions and Spectral Line Shifts*

William S. Cooper III and Heinz Ringler†
Lawrence Radiation Laboratory, University of California, Berkeley, California 94720
(Received 3 October 1968)

We have observed normally forbidden two-quantum transitions in the optical spectrum of a helium plasma. We induced these transitions by applying a microwave field to a separately generated steady-state helium discharge. Measurements of the relative intensity and wavelength of the optical photons emitted in the two-quantum transition $5^1F^0 \rightarrow 2^1P^0$ in He I determined both the frequency and the strength of the microwave field in the plasma. The field strength was also measured by observation of the Stark shift of a spectral line and by measurement of the microwave power input and the Q of the microwave cavity. All measurements of the field strength are in satisfactory agreement and indicate an rms microwave field strength in the plasma of about 215 V/cm. The spectroscopic measurement of the frequency of the microwave field is within 3% of the actual value, and the measured polarization of the radiation agrees with theory.

I. INTRODUCTION

An oscillating electric field has certain observable effects on the spectrum of radiation emitted by excited atoms. These effects can, in principle, be used to measure the frequency, strength, and direction of the electric field. If the radiating atoms are located in a plasma, these effects provide the important possibility of studying the electric fields in the plasma by spectroscopic techniques. Two advantages of spectroscopic methods are obvious: first, the plasma is not perturbed by the measurement, and second, the frequency response is sufficient to observe even the most rapid plasma phenomena. The disadvantages are first, that it is difficult to localize the measurement unless the plasma is cylindrically symmetric, so that one may use Abel inversion,[1] and second, fairly strong fields may be required to produce measurable effects.

The theory of the linear Stark effect in a rapidly varying electric field has been discussed by Schrödinger,[2] and by Blochinzew[3] for the particular case of a sinusoidally varying electric field. The effect on a spectral line which exhibits a linear Stark effect is a modification of the line profile which, if competing line-broadening mechanisms are not too large, may be used to measure the strength and, in some cases, the frequency of the perturbing electric field. This technique has been used to measure the strength of an externally applied microwave field in a plasma[4] and to measure the strength of stochastic fields in a beam-plasma interaction experiment.[5] Both experiments were in hydrogen, and in neither case was information about the frequency spectrum of the fields derived from the measurements.

In nonhydrogenic atoms, a sinusoidally varying electric field can induce normally forbidden two-quantum transitions involving emission or absorption of one quantum from the field plus emission of an optical photon. This effect was proposed by

Baranger and Mozer as a means of observing longitudinal plasma oscillations,[6] and has also been treated by Reinheimer as an absorption process.[7] We have used these transitions to measure both the frequency and the strength of a microwave field externally applied to a helium plasma. In addition, we measured the strength of the microwave electric field in the plasma by observing the shift of a spectral line resulting from an allowed transition – analogous to the line-profile measurements in hydrogen described in Ref. 4 and 5.

II. THEORY

We shall discuss briefly the perturbation treatment which leads to the theoretical expression for the intensity of the two-quantum transitions. Suppose that we have an excited nonhydrogenic atom in some initial state i, and that the atom is situated in an oscillating electric field with amplitude E and angular frequency ω. What is the probability per unit time that at some later time the atom has made a transition to a specific final state k? The following two-quantum process can occur: the atom either absorbs one quantum of energy $\hbar\omega$ from the field or emits one quantum to the field. The atom exists transiently in a virtual state separated in energy by $\pm\hbar\omega$ from the initial state, and then makes a transition to the final state k by emitting an optical photon with frequency $\omega_{ik} \pm \omega$. Here ω_{ik} is the angular frequency of transitions between states i and k. Figure 1 shows the energy levels i and k, a representative intermediate state j, the virtual states (shown by dashed lines), and the transitions between them.

A. Probability of Two-Quantum Transitions

The probability per unit time that such a transition will occur can be calculated by second-order time-dependent perturbation theory. The final result of such a calculation averaged over all possible field directions is given in Ref. 6, and a sketch of the derivation is given in Ref. 7. The selection rules are such that the transition from i to k by emission of a single photon is forbidden in the electric-dipole approximation; the effect of these two-quantum transitions on the optical spectrum is the appearance of "satellites" separated in frequency by $\pm\omega$ from ω_{ik}, the frequency of the forbidden direct transition from i to k. The satellites are indicated in Fig. 2, which shows schematically the intensity of the emitted radiation in the vicinity of ω_{ik}.

In our experiment the oscillating electric field which induces the two-quantum transitions is not random in direction, but is directed perpendicular to the direction of observation of the satellites. As stated in Ref. 6, the satellites in this case will be emitted anisotropically and will also

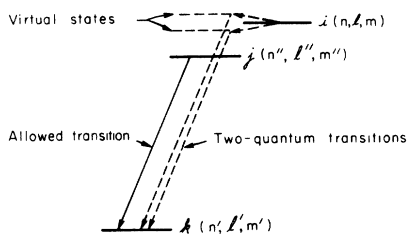

FIG. 1. Partial term diagram, showing an allowed transition and two-quantum transitions via virtual states. The figure is drawn schematically for $l \rightarrow l-2$ transitions.

be polarized. We must therefore look at the expression for the transition probabilities *before* averaging over all field directions, so that we can calculate the anisotropy and polarization of the satellites. The perturbation treatment outlined in Ref. 6 and 7 leads to the following expression for the differential transition probability:

$$dA_i^k = (e^2/8\pi\hbar^3c^3)(\omega_{ik} \pm \omega) \times \sum_j [\omega_{jk}/(\omega_{ij} \pm \omega)]^2 |V_i^j|^2 |\xi_j^k|^2 d\Omega , \quad (1)$$

where dA_i^k is the differential probability per second for a two-quantum transition from i to k, resulting in the emission of a photon into solid angle $d\Omega$; ω_{ij} is the angular frequency of a transition from i to j; ω_{ik} is the angular frequency of a transition from i to k; ω_{jk} is the angular frequency of a transition from j to k. In Eq. (1), V_i^j, the matrix element of the perturbation taken between states i and j, is given in the dipole approximation by

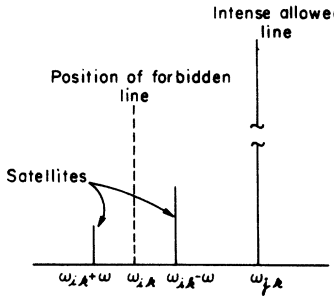

FIG. 2. The spectrum in the vicinity of the transitions shown in Fig. 1, drawn for wavelength increasing toward the right.

$$V_i^j = \int \psi_j^* e\vec{\mathbf{E}} \cdot \vec{\mathbf{r}} \psi_i d^3x , \tag{2}$$

and ξ_j^k is a matrix element between states j and k, defined by

$$\xi_j^k = \int \psi_k^* \vec{\mathbf{r}} \cdot \vec{\mathbf{a}} \psi_j d^3x , \tag{3}$$

where $\vec{\mathbf{r}}$ is the position vector of the electron, and $\vec{\mathbf{a}}$ is a unit vector in the direction of polarization (assumed to be linear) of the emitted photon. The plus sign is to be used in Eq. (1) if a quantum of energy from the field is absorbed; the minus sign if a quantum of energy is emitted to the field. The sum is over all intermediate states. We assume the electric field to be only in the $\vec{\mathbf{z}}$ direction; then

$$|V_i^j|^2 = 2e^2 E_{\text{rms}}^2 |z_i^j|^2 . \tag{4}$$

Information about the polarization and angular dependence of emission is contained in $|\xi_j^k|^2$. Suppose the photon is emitted at an angle θ with respect to the electric field. Then one can show[8,9] that for polarization parallel to the field,

$$|\xi_j^k|^2 \equiv |\pi_j^k|^2 = (|x_j^k|^2 + |y_j^k|^2)\tfrac{1}{2}\cos^2\theta + |z_j^k|^2 \sin^2\theta , \tag{5}$$

and for polarization perpendicular to the field,

$$|\xi_j^k|^2 \equiv |\sigma_j^k|^2 = \tfrac{1}{2}(|x_j^k|^2 + |y_j^k|^2) . \tag{6}$$

The matrix elements x_j^k, y_j^k, and z_j^k are the matrix elements of the corresponding coordinates; expressions for them are given (in the Coulomb approximation) in Ref. 10.

Now we replace the i, j, k designation in the matrix elements with sets of quantum numbers: $i \to (n,l,m)$; $j \to (n'',l'',m'')$, and $k \to (n',l',m')$. We find the following set of selection rules after we evaluate the terms in the sum:

$$l'' = l \pm 1 ,$$

$$l' = l'' \pm 1 = l \text{ or } l \pm 2 ,$$

and $$m'' = m .$$

Because of the resonant denominator in Eq. (1), the only intermediate states that can contribute significantly to the sum are those lying very close in energy to the state i; we therefore also assume

$$n'' = n .$$

(This assumption may not be true in general.) From now on, we consider *only* transitions of the type $l \to l \pm 2$.

To get an expression for the differential transition probability regardless of the polarization, we first sum Eq. (1) over both polarizations. Equation (1) is now a sum over m and m', but since the usual definition of the transition probability is the probability per m state, we must also divide the expression by the statistical weight of the ith level, namely g_i. After carrying out these indicated operations and changing the labeling of the states, we have an expression for the differential probability of transitions from the state (n,l) to the state (n',l'):

$$dA_{nl}^{n'l'}(\theta) = \frac{1}{4\pi} \frac{e^4 E_{\text{rms}}^2}{\hbar^3 c^3} \frac{(\omega_{ik} \pm \omega)\omega_{jk}^2}{(\omega_{ij} \pm \omega)^2} \times (1/g_i) \sum_{m,m'} |z_{nlm}^{nl''m}|^2 \times (|\pi_{nl''m}^{n'l'm'}|^2 + |\sigma_{nl''m}^{n'l'm'}|^2) d\Omega . \tag{7}$$

For simplicity, we have retained the (i,j,k) notation in labeling ω. We assume that none of the frequencies depend on m, m', or m''; that is, we neglect Stark shifts. For example, ω_{ik} denotes the frequency of the transition between state (n,l) and state (n',l').

The indicated sums can be worked out, using expressions given in Ref. 10 for the necessary matrix elements (Coulomb approximation) to give in the case $l \to l-2$,

$$\sum_{m,m'} |z_{nlm}^{n\,l-1\,m}|^2 |\pi_{n\,l-1\,m}^{n'\,l-2\,m'}|^2 = \frac{2}{15} \frac{l(l-1)}{(2l-1)} |R_{nl}^{n\,l-1}|^2 |R_{n\,l-1}^{n'\,l-2}|^2 \times (\sin^2\theta + \tfrac{3}{4}\cos^2\theta) , \tag{8}$$

and

$$\sum_{m,m'} |z_{nlm}^{n\,l-1\,m}|^2 |\sigma_{n\,l-1\,m}^{n'\,l-2\,m'}|^2 = \frac{1}{10} \frac{l(l-1)}{(2l-1)} |R_{nl}^{n\,l-1}|^2 |R_{n\,l-1}^{n'\,l-2}|^2 . \tag{9}$$

For $l \to l+2$, we have

$$\sum_{m,m'} |z_{nlm}^{n\,l+1\,m}|^2 |\pi_{n\,l+1\,m}^{n'\,l+2\,m'}|^2 = \frac{2}{15} \frac{(l+1)(l+2)}{(2l+3)} |R_{nl}^{n\,l+1}|^2 |R_{n\,l+1}^{n'\,l+2}|^2 \times (\sin^2\theta + \tfrac{3}{4}\cos^2\theta) , \tag{10}$$

and

$$\sum_{m,m'} |z_{nlm}^{\,n\,l+1\,m}|^2 |\sigma_{n\,l+1\,m}^{\,n'l+2\,m'}|^2 = \frac{1}{10}\frac{(l+1)(l+2)}{(2l+3)} |R_{nl}^{\,n\,l+1}|^2 |R_{n\,l+1}^{\,n'l+2}|^2 . \tag{11}$$

Here $R_{nl}^{\,n'l'}$ is an integral over the radial eigenfunctions, defined by[11]

$$R_{nl}^{\,n'l'} = \int R_{n'l'}(r) R_{nl}(r) r^3 dr . \tag{12}$$

Equations (8) through (11) can be used to calculate the differential transition probability for a given transition. Before we continue with this calculation, however, let us first calculate the anisotropy of the radiation pattern and the polarization of a satellite.

B. Anisotropy of the Radiation Pattern of the Satellites

Note from Eqs. (7) through (11) that for both $l \to l-2$ and $l \to l+2$, we have

$$dA(\theta) \propto [\sin^2\theta + \tfrac{3}{4}(1+\cos^2\theta)] . \tag{13}$$

Now we average the differential transition probability over all angles of emission (or, equivalently, over all possible field directions, for a fixed direction of observation) to obtain

$$\overline{dA} \equiv (1/4\pi) \int dA(\theta) d\Omega . \tag{14}$$

The relative anisotropy of emission is then given by

$$dA(\theta)/\overline{dA} = \tfrac{3}{5}[\sin^2\theta + \tfrac{3}{4}(1+\cos^2\theta)] . \tag{15}$$

For $\theta = \pi/2$, which was the case in our experiment, the intensity of a satellite exceeds the average intensity by 5%.

C. Polarization of the Satellites

The intensity of radiation is proportional to

$$\sum_{m,m'} |z|^2 |\pi|^2$$

for polarization parallel to $\vec{E}$, and to

$$\sum_{m,m'} |z|^2 |\sigma|^2$$

for polarization perpendicular to $\vec{E}$. We define the fractional polarization parallel to $\vec{E}$ by

$$P(\theta) \equiv \frac{\sum |z|^2|\pi|^2 - \sum |z|^2|\sigma|^2}{\sum |z|^2|\pi|^2 + \sum |z|^2|\sigma|^2} . \tag{16}$$

Using Eqs. (8) through (11) we find for either $l \to l-2$ or $l \to l+2$ transitions

$$P(\theta) = \frac{\sin^2\theta + \frac{3}{4}\cos^2\theta - \frac{3}{4}}{\sin^2\theta + \frac{3}{4}\cos^2\theta + \frac{3}{4}} = \frac{\sin^2\theta}{6 + \sin^2\theta} . \tag{17}$$

The maximum polarization occurs for $\theta = \pi/2$, the conditions of our experiment, and in this case the polarization is $\frac{1}{7}$.

D. Ratio of the Intensity of a Satellite to the Intensity of an Allowed Line

It is convenient both to calculate from the theoretical point of view and to measure from the experimental point of view, not the absolute intensity of a satellite, but rather the *ratio* of the intensity of a satellite to the intensity of the nearby allowed line resulting from the transition $j \to k$. The intensity of either the satellite or the allowed line is proportional to the frequency of the transition and to the density of atoms in the upper state of the transition. This intensity ratio, which we call $S_{\pm}(\theta)$ is

$$S_{\pm}(\theta) = (\omega_{ik} \pm \omega) N_i dA_i^{\,k} / \omega_{jk} N_j dA_j^{\,k} , \tag{18}$$

where N_i is the density of atoms in the state i, N_j is the density of atoms in the state j, and $dA_j^{\,k}$ is the differential probability per second of a spontaneous transition from state j to state k into solid angle $d\Omega$, summed over both polarizations. The expression for $dA_j^{\,k}$ is[12]

$$dA_j^{\,k} = (\omega_{jk}^{\,3}/2\pi\hbar c^3)(|\pi_j^{\,k}|^2 + |\sigma_j^{\,k}|^2) d\Omega . \tag{19}$$

As before, we work out the appropriate sums over m and m', and divide by the statistical weight of the jth state g_j to obtain for $l-1 \to l-2$

$$dA_{n\,l-1}^{\,n'l-2} = (e^2\omega_{jk}^{\,3}/3\pi\hbar c^3)(1/g_j) \times (l-1)|R_{n\,l-1}^{\,n'l-2}|^2 d\Omega , \tag{20}$$

and for $l+1 \to l+2$

$$dA_{n\,l+1}^{\,n'l+2} = (e^2\omega_{jk}^{\,3}/3\pi\hbar c^3)(1/g_j) \times (l+2)|R_{n\,l+1}^{\,n'l+2}|^2 d\Omega . \tag{21}$$

Note that these differential transition probabilities are independent of θ; the radiation pattern of the allowed line remains isotropic in the presence of the electric field.

Assume the excited states to be in thermal equilibrium at temperature T, so that N_i and N_j are related by a Boltzmann factor

$$N_i/N_j = (g_i/g_j)\exp[-(E_i - E_j)/kT] , \quad (22)$$

where E_i is the energy of state i and E_j is the energy of state j, both measured from the ground state. We can now calculate $S_\pm(\theta)$, which we express in the form

$$S_\pm(\theta) = \frac{1}{10}\frac{e^2 a_0^2}{\hbar^2}\frac{E_{\rm rms}^2}{(\omega_{ij}\pm\omega)^2}\left(\frac{\omega_{ik}\pm\omega}{\omega_{jk}}\right)^2 \times \mathcal{R}_{ll'}[\sin^2\theta + \tfrac{3}{4}(1+\cos^2\theta)] \times \exp[-(E_i - E_j)/kT] . \quad (23)$$

Here we have, for $l \to l-2$,

$$\mathcal{R}_{ll'} = [l/(2l-1)a_0^2]\,|R_{nl}^{\,n\,l-1}|^2 = \tfrac{9}{4}[l/(2l-1)]n^2(n^2-l^2) , \quad (24)$$

and for $l \to l+2$,

$$\mathcal{R}_{ll'} = [(l+1)/(2l+3)a_0^2]\,|R_{nl}^{\,n'\,l+1}|^2 = \tfrac{9}{4}[(l+1)/(2l+3)]n^2[n^2-(l+1)^2] , \quad (25)$$

where a_0 is the Bohr radius, and $\mathcal{R}_{ll'}$ is the same dimensionless quantity defined in Eq. (2) of Ref. 6, except that we have interchanged the definitions of l and l'.

If the electric field is random in direction, we must average our Eq. (23) over all directions, just as we did in the case of the differential transition probability, to obtain the average intensity ratio $\bar{S}_\pm$. If we assume that the upper states are so close together that

$$[(\omega_{ik}\pm\omega)/\omega_{jk}]^2 \cong 1, \quad \text{and } (E_i - E_j)/kT \ll 1,$$

we have

$$\bar{S}_\pm = (e^2 a_0^2/6\hbar^2)E_{\rm rms}^2\mathcal{R}_{ll'}/(\omega_{ij}\pm\omega)^2 , \quad (26)$$

which is the same as Eq. (1) of Ref. 6. A restriction, due to the use of perturbation theory, is that $S_\pm(\theta)$ or $\bar{S}_\pm$ must be much smaller than one.

A major difficulty in attempting to measure the intensity ratio S arises from the fact that both the satellites and the allowed line exhibit broadening, which may be real or instrumental. The satellites are superimposed on the wing of the allowed line, which tends to obscure them and make their detection more difficult.

The potential of these two-quantum transitions in plasma spectroscopy is now obvious from Eq. (26) and Fig. 2. By measurement of the wavelength separation of the satellites, it should be possible to measure the frequency of fluctuating electric fields in the plasma and, by relative intensity measurements, the electrostatic energy density in the fluctuations. By suitable unfolding of the measured spectrum, one could obtain the power spectrum of fluctuating electric fields in a plasma by a technique which does not perturb the plasma and has arbitrarily high frequency response. The experiment described in the following section was designed to test the feasibility of this method for studying electric fields in plasmas.

III. EXPERIMENT

A. Apparatus

An experiment designed to study the production of these satellites should satisfy the following conditions: (1) the apparatus should produce a stable, steady-state helium plasma; (2) it should be possible to produce within this plasma an electric field that can be modulated and which has a known direction, intensity, and frequency; (3) the intensity of the field should be sufficiently large that the satellites can be detected in the presence of the superimposed wing of the allowed line; (4) the frequency of the field should be high enough that the wavelength separation of the satellites is larger than the resolution of the spectrometer to be used and (5) the electric field should have a negligible effect on the plasma properties (electron density, temperature, and density of excited states). Figure 3 shows a schematic diagram of an experiment that satisfied these requirements.

A helium plasma was produced by a dc discharge between tungsten electrodes in a small quartz discharge tube. The outer diameter of the discharge tube was 1 mm, the inner diameter about $\frac{1}{3}$ mm, and the length of the capillary section 7.8 cm. Helium was admitted at pressures ranging from 20 to 100 Torr at one end of the tube; the other end of the tube was connected through a liquid-

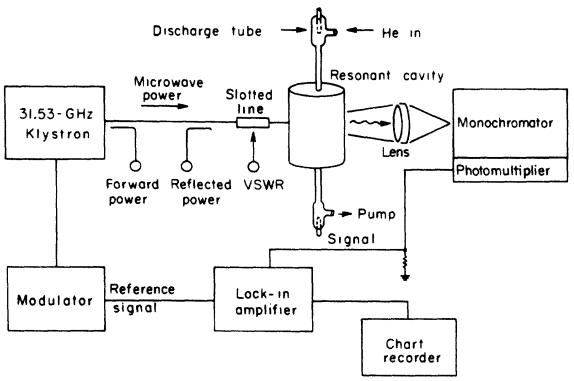

FIG. 3. Schematic diagram of the experiment.

nitrogen-cooled trap to a mechanical pump, so that helium flowed continuously through the tube. The electrode in the high-pressure end of the tube was connected through a 3-MΩ resistor to the negative terminal of a high-voltage power supply capable of putting out 3 mA at 15 kV.

The discharge tube passed completely through a cylindrical microwave cavity, along the axis of symmetry of the cavity. The cavity, machined in a split block of brass, was 0.662 cm diam and 0.929 cm long. The first version was silver plated, but the silver plating was quickly destroyed when the discharge tube was turned on, presumably because of oxidation by atomic oxygen or ozone produced by ultraviolet radiation escaping through the thin quartz walls of the discharge tube. The final version was gold plated, and was also continuously flushed with dry nitrogen during operation of the discharge tube, preventing further trouble due to oxidation. The cavity was excited in the TM_{010} mode at 31.53 GHz by an OKI model-35V10 klystron, providing a high-frequency electric field of known direction, strength, and frequency in the plasma. The mode identification was verified by calculating the resonant frequency, which was within 1% of the observed value, and by locating the TM_{011} mode at 35.83 GHz, also within about 1% of the calculated frequency.

We were able to monitor the frequency of the microwaves, the power put out by the klystron, and the voltage standing-wave ratio (VSWR) near the cavity, which was coupled to the end of the waveguide by an iris. Measurement of the attenuation in the waveguide allowed us to calculate the value of each quantity at the cavity; measurement of these quantities as the frequency of the klystron was changed enabled us to determine the resonant frequency and the Q of the system for various values of the discharge parameters. These measurements indicated that for the usual conditions of operation of the discharge tube the electron-collision frequency for momentum transfer ν_c and the plasma frequency ω_p are related to ω by $(\nu_c/\omega) \approx (\omega_p/\omega)^2 \approx 0.1$. This indicates that the microwave field should have very little effect on the plasma other than stimulation of the desired two-quantum transitions in its emission spectrum. Typical conditions in the discharge at the location of the cavity (2.7 cm from the low-pressure end of the tube) were 8-Torr pressure, 3-mA current, 3.4-A/cm^2 current density, about 175-V/cm dc electric field driving the current, 1.2×10^{12} cm^{-3} electron density, and an average electron energy of about 10 eV.

Light from within the cavity passed through a narrow slit in the wall, was collected by a lens and was focused onto the entrance slit of a JACO model 82-000 0.5-m monochromator. The resolution of this instrument (full width at half maximum) with the 10-μ-wide slits used was about 0.2 Å, ample to resolve the two satellites, whose expected separation in the visible region of the spectrum was about 0.4 Å. Detection was done photoelectrically with an uncooled EMI 6256-S photomultiplier; the linearity of the photomultiplier was checked in a separate experiment.

The instrument function of the monochromator has rather broad wings. This fact, together with the contribution from collision broadening of the allowed line, produced a "continuum" in the vicinity of the satellites which was 5 to 10 times brighter than the satellites themselves. We were able to discriminate against this large unwanted dc signal by square-wave modulating ("chopping") the microwave power at 1 kc/sec (the discharge ran continuously and steadily) and using synchronous detection.

The signal from the photomultiplier was fed into a PAR Model HR-8 lock-in amplifier, which used a signal from the klystron modulator as a reference signal. In this way we could measure the component of the photomultiplier signal which was synchronous with and in phase with the chopped microwave signal at a number of discrete wavelengths in the spectral region near the allowed lines, and ignore features in the spectrum which were not produced by the microwave field in the plasma. The wavelength of observation was changed in small and reproducible increments by tilting a quartz plate installed for this purpose just behind (i.e., on the grating side of) the exit slit of the monochromator. At each wavelength, the output of the lock-in amplifier (time constant 10 sec) was recorded with a chart recorder (time response 0.1 sec) for 5 to 10 min; the amplitude of the resulting trace was later measured at intervals corresponding to 30 sec of recording time, and these measurements averaged to give one data point. At each wavelength we also switched the photomultiplier signal briefly to a Keithley Model 410 micromicroammeter to measure the dc component of the signal.

B. The Data and Data Reduction

Figure 4 shows the measurements of the component of the photomultiplier signal which was synchronous with and in phase with the chopped microwave signal in the vicinity of the allowed 4387.93-Å He I line ($5^1D \rightarrow 2^1P^0$) and the forbidden 4387.36-Å He I line ($5^1F^0 \rightarrow 2^1P^0$). The abscissa in Fig. 4 is $\Delta\lambda$, the separation in Å from the center of the allowed line. The data were taken on two different days. The satellites are evident; arrows indicate their theoretical positions, as calculated from the measured microwave frequency and the term values for He I given by Martin.[13]

There is also an additional, large, asymmetric signal centered near $\Delta\lambda = 0$. This signal is caused by the Stark *shift* of the 4387.93-Å He I allowed

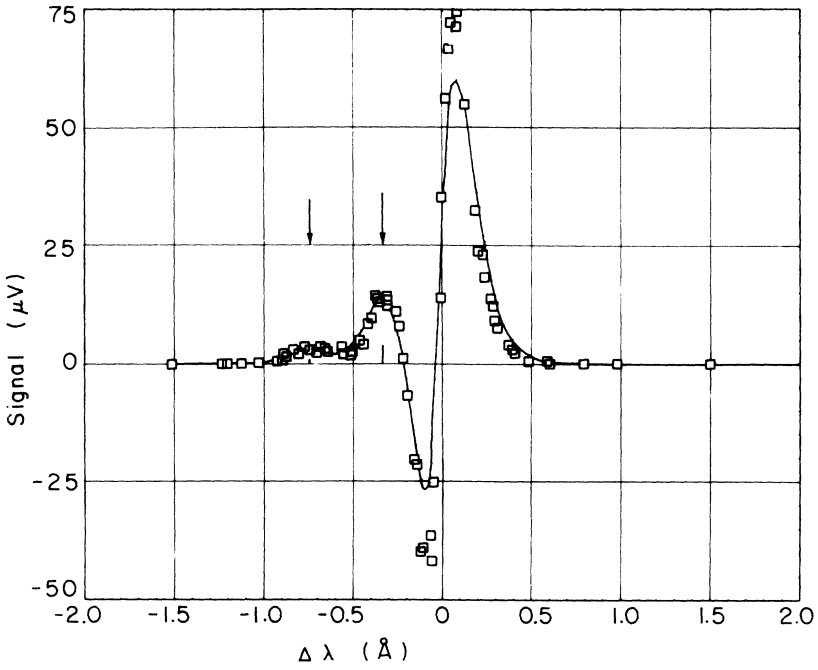

FIG. 4. The measured signal as a function of the wavelength separation from the center of the allowed line.

line, and provides an independent method of measuring the rms electric field in the plasma. Suppose we measure the apparent profile (almost entirely instrumental in this case) of the 4387.93-Å line with no microwave power in the cavity. The sign of the Stark-shift coefficient for the 5^1D level is negative; therefore, if we switch on an electric field, this line will shift toward the red. The amount of the shift is proportional to the square of the applied field, provided the field is not too large. If the monochromator is set on the red wing of this line, when the field is applied the photomultiplier signal will increase; for settings on the blue wing of the line the signal will decrease. For alternating electric fields with frequencies high enough that $\hbar\omega$ is much larger than the Stark shift and much smaller than the energy separation from the next level (these conditions are satisfied in our case), the Stark shift may be calculated using the theory for static fields and the rms value of the alternating field.[14] It is clear that if we chop the microwave power in the cavity, the lock-in amplifier will see a positive signal on the red wing of the line and a negative signal on the blue wing. We can calculate this signal, which is the rms value of the Fourier component of the difference signal, by assuming that the shift is much less than the apparent width of the line, and expanding the line profile in a Taylor series about the line center. We have carried out this calculation in the general case, allowing also for the existence of a dc electric field E_0 and a linear Stark shift. The result, the rms signal observed by the lock-in amplifier, is

$$\begin{aligned}\text{Sig} = 0.45 I_0 \sum_i \epsilon_i \{ &- F' \beta_i E_{\text{rms}}^2 \\ &+ \tfrac{1}{2} F'' [\alpha_i^2 E_{\text{rms}}^2 \\ &+ \beta_i^2 (6 E_0^2 E_{\text{rms}}^2 + \tfrac{3}{2} E_{\text{rms}}^4)] + \cdots \} , \end{aligned} \quad (27)$$

where F is the instrument function, normalized according to

$$\int_{-\infty}^{\infty} F(\Delta\lambda) d(\Delta\lambda) = 1 , \quad (28)$$

α_i and β_i are the linear and quadratic Stark coefficients of the ith component of the line, defined by

$$\Delta\lambda = \alpha_i E + \beta_i E^2 , \quad (29)$$

ϵ_i is the intensity of the ith component, normalized according to

$$\sum \epsilon_i = 1 , \quad (30)$$

(ϵ_i is a function of the angle of emission with respect to the electric field), and I_0 is the integrated intensity of the line. For helium, of course, α_i is zero. In our case the fields are small enough that only the first term in the sum contributes significantly, and the observed signal due to the Stark shift of the allowed line is proportional to the first derivative of the instrument function. The intensity of the forbidden line is so small relative to the allowed line that the signal due

to its Stark shift is negligible.

The signal given by Eq. (27) complicates the measurement of the intensities of the satellites, because it partially overlaps the red satellite. There is, in addition, a further complication. Even a slight modulation of the *intensity* of the very intense allowed line in phase with the microwave modulation can produce a measurable signal. This modulation could arise, for example, from a slight increase in the electron temperature during the microwave pulse, which in turn increases the density of 5^1D states. In the analysis of the data in Fig. 4, we must allow for this possibility also. This signal also partially overlaps the red satellite.

To unfold the observed signal shown in Fig. 4 into its various components, we used a computer program developed by K. Halbach of this laboratory[15] to fit to the data, in a least-squares sense, signals having the shape of the instrument function or its first derivative. Four signals were specified: (1) a signal with the shape of the instrument function located near the blue satellite; (2) the same, but located near the red satellite; (3) the same, near $\Delta\lambda = 0$, to account for the modulation of the allowed line; and (4) a signal proportional to the first derivative of the measured instrument function, located at the same wavelength as (3). The signals were varied in both amplitude and wavelength until a best fit to the data was obtained; the sum of all four signals is shown by the solid curve in Fig. 4. The fit, especially to the satellites, is quite good. The positions and relative intensities of the satellites are indicated by the short dark lines.

Within the accuracy of measurement, the measured profiles of the satellites and of the allowed line were identical, and were very nearly identical to the instrument function. We may therefore calculate the desired intensity ratios $S_{\pm}(\theta)$ by comparing the peak intensities of the various lines, as determined by the computer fitting procedure, after correcting for the fact that the measured frequency response of the detecting system at 1 kHz was 0.84 of the dc value. (Note that this in no way limits the capacity to measure the frequency of electric fields in the plasma, as this measurement is based on a spectroscopic measurement of the wavelength separation of the satellites.) The peak intensity of the satellites was remarkably constant in time, but the peak intensity of the allowed line drifted upward by about 40% during the course of a day's run, which typically lasted 6 or 7 h. The parameters of the discharge tube remained constant to a few percent during this time, and subsequent experiments showed that the gain of the detecting system also remained constant. We used the mean value, with an uncertainty of 20%, in calculating the intensity ratios, and have no explanation for the drift.

The analysis of the data contained in Fig. 4 and in the dc measurements of the allowed line intensity may be summarized as follows:

(1) The measured separation of the satellites is 0.417 Å. (2) The ratio of the intensity of the blue satellite to the intensity of the allowed line, S_+, is 6.7×10^{-4}. (3) The ratio of the intensity of the red satellite to the intensity of the allowed line, S_-, is 2.7×10^{-3}. (4) The rms shift of the allowed line due to the microwave field is 0.0013 Å to the red. (5) The fractional modulation of the allowed line due to the microwave field is 0.007.

IV. RESULTS

We present the results as a comparison of the spectroscopically measured microwave frequency with the known frequency, a comparison of the several spectroscopic measurements of the rms electric field strength in the plasma with the value derived from microwave measurements, and a comparison of the measured polarization of one satellite with the theoretical value.

A. Frequency Measurements

Using the measured separation of the satellites of 0.417 ± 0.02 Å (error estimated) and knowing the wavelength (4387.4 Å), we calculate the frequency of the field in the plasma to be 32.5 ± 1.6 GHz. The average of two direct measurements of the microwave frequency with two different cavity wavemeters was 31.565 GHz. The discrepancy is less than 3%, well within the estimated error.

B. Electric-Field Measurements

Using Eq. (23), evaluated for this transition and for $\theta = \pi/2$, $T = \infty$, we obtain from the ratio of the intensity of the blue satellite to that of the allowed line an rms electric field in the plasma of 252 ± 30 V/cm, and from the ratio of the intensity of the red satellite to that of the allowed line, a value of 242 ± 30 V/cm. The error estimates result from the assumption of reasonable errors (assumed to be independent) in measuring the intensities of the satellites and of the allowed line, the frequency response of the system at 1 kHz relative to the dc response, and the use of the Coulomb approximation in evaluating the radial matrix element in $\mathcal{R}_{ll'}$. The assumption of infinite temperature, equivalent to the assumption that the upper states of the transitions are populated in proportion to their statistical weights, will be discussed later.

The computer analysis of the data yielded directly the amount of signal in Fig. 4 which was proportional to the first derivative of the instrument function. We could therefore obtain an in-

dependent measure of the rms electric field in the plasma from Eq. (27), which relates this signal to the Stark shift. As already mentioned, in this case only the first term in this equation is significant (this can be justified *a posteriori*). The intensity coefficients ϵ_i of the various components of the line (different magnetic quantum numbers) depend on the angle of emission with respect to the electric field. Using calculations similar to those presented in Sec. II with Stark-shift coefficients from Bethe and Salpeter,[16] and evaluating the results for $\theta = \pi/2$, we obtain a value of 228 ± 35 V/cm for the rms electric field in the plasma as measured by this method.

We can calculate a final value of the electric field in the plasma from the microwave data. The measured loaded Q of the system of cavity, quartz tube, and plasma under the usual operating conditions was 1005 ± 120. This is an average of measurements by two different methods. In the first, we measured the VSWR in a section of slotted line about 40 cm from the cavity as a function of frequency around the resonant frequency. We also measured the attenuation of the connecting waveguide as a function of frequency. Using known methods[17] we then calculated both the loaded Q of the cavity and the coupling coefficient, which was 1.50. The other method of measuring the Q of the system was to measure, with a horn antenna and a crystal detector, the signal radiated by the slit of the cavity through which the light emerged. We measured this signal also as a function of frequency around the resonant frequency, assumed that it was proportional to the energy stored in the cavity, and calculated a value of Q from its halfwidth. The two methods gave results that are in reasonable agreement. The peak microwave power at the cavity was measured indirectly with a Hewlett-Packard Model 431 C power meter and directly with a PRD Model 666 dry calorimeter. The results were in excellent agreement, and indicated a peak power into the cavity of 50.6 mW (a small correction was made for the reflected power). This is sufficient to calculate the total stored energy from the definition of Q. It remains to relate this quantity to the electric field in the plasma. This was done by solving numerically the boundary-value problem of plasma, quartz tube, and cavity for the TM_{010} mode, neglecting the apertures at the ends of the cavity through which the discharge tube passed. We feel that the effect of these apertures is not too important, as the calculated resonant frequency was within 1% of the observed value. The final result of these measurements and calculations was 193 ± 17 V/cm for the rms electric field in the plasma. All four measurements of the electric field are summarized in Table I.

The weighted mean value of the rms electric field from the spectroscopic measurements is about 25% higher than the value derived from microwave measurements. In view of the estimated errors, which range from 9 to 15% and include only estimated random errors, it is difficult to say whether this discrepancy is real. There may be a systematic error in the electric-field-strength measurements from the ratio of the satellite intensities to the intensity of the allowed line. These measurements depend on the assumption that the upper states involved, the $5\,^1D$ and $5\,^1F^0$ states, are populated according to their statistical weights. This may not be the case in helium discharges of this type, because different mechanisms may populate (or depopulate) the states, causing a lack of detailed balancing and a departure of the population densities from the value expected for thermal equilibrium. The degree of ionization in our plasma at the point of observation is only about 5×10^{-6}, which means that atom-atom collisions can play important roles in governing the populations of the excited states. Because of the high neutral density, one would expect the ^1P states to be closely coupled to the ground state because of the trapping of resonance radiation. The cross section for the transfer of excitation energy from ^1P states to $^{1,3}F$ states by atom-atom collisions is known to be very large.[18] This process may govern the population of the ^1F states (the upper state of the forbidden line and the satellites), whereas the population of the ^1D states (the upper state of the allowed line) may be determined by other processes, such as inelastic electron-atom collisions and radiative transitions. The possibility clearly exists for the failure of Eq. (22) to predict the ratio of the densities of the excited states. A departure of about 50% from the expected ratio would be sufficient to bring all measurements of the electric-field strength into excellent agreement.

TABLE I. Summary of electric field measurements.

Method	rms electric field in the plasma (V/cm)
Microwave data	193 ± 17
Red satellite	242 ± 30
Blue satellite	252 ± 30
Shift of allowed line	228 ± 35

We measured the relative densities of the $4\,^1S$, $4\,^1P^0$, $4\,^1D$, $4\,^3S$, $4\,^3D$, $5\,^1S$, $5\,^1D$, $5\,^3S$, $5\,^3D$, and $6\,^1D$ states to determine whether there were significant departures of the excited state populations from equilibrium values. These measurements were carried out by measuring the relative intensities of spectral lines originating from these states, after first calibrating the relative sensitivity of the detecting instruments with a standard lamp. The relative intensity I of a spectral line is proportional to $(gA/\lambda)\exp(-E/kT)$, where g is the statistical weight of the upper level, E is the energy

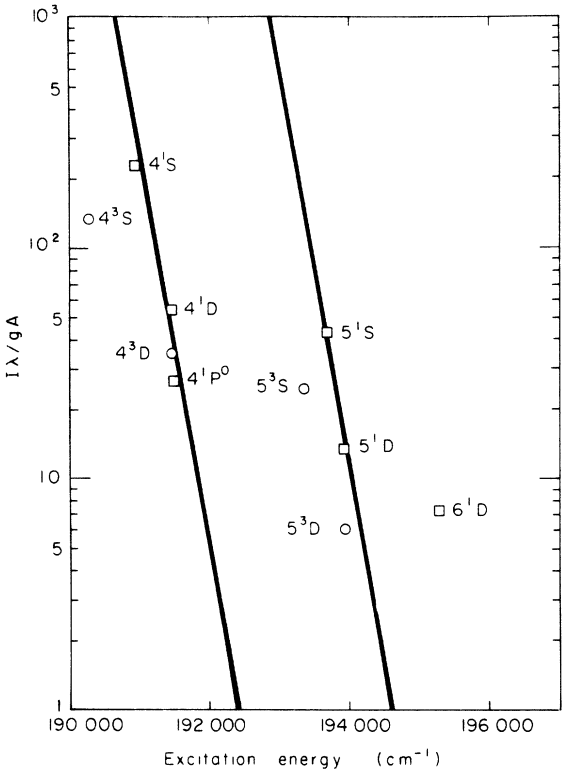

FIG. 5. Relative population density of He I excited states in the discharge as a function of the excitation energy of the state.

of this level, A is the transition probability, and λ is the wavelength of the line. A plot of $\ln(I\lambda/gA)$ versus E should, in the case of thermal equilibrium, yield a straight line with a slope of $-1/kT$.

Figure 5 shows the measured values of $(I\lambda/gA)$ for the states mentioned above on a semilogarithmic plot against the term values of the states. There are clearly large departures from thermal equilibrium. It appears, however, the densities of all singlet states for a given principal quantum number can be described by a temperature, although there is no obvious relationship between the densities of singlet states with different principal quantum numbers, or to any of the triplet states. The figure shows two straight lines having the same slope, one drawn through the points representing the singlet states with $n=4$ and the other through the points representing the singlet states with $n=5$. The slope of these lines represents a temperature of 360°K, which is very reasonable for the gas temperature, and indicates that atom-atom collisions play an important role in determining the population of these states. Unfortunately, we could not observe the infrared allowed transitions from the 5^1F^0 state, and so could not directly measure the ratio of the densities of the two states important in our experiment. The fact that the intensity of the allowed line varied slowly with time, whereas the intensity of the satellites remained reasonably constant probably indicates a departure from the equilibrium ratio, as this drift was far too large to be explained by variation in the gas temperature alone.

C. Polarization Measurements

The discharge tube was damaged before we were able to make polarization measurements of the satellites of the $5^1F^0 - 2^1P^0$ forbidden line. However, the theory predicts identical polarizations for all two-quantum transitions satisfying $l \to l \pm 2$. We had measured the polarization of the red satellite of the $4^1F^0 - 2^1P^0$ transition during some preliminary work on this transition, and found the satellite to be slightly polarized in the direction of the applied field. The π and σ components of the polarization were measured with the aid of a Polaroid filter adjacent to the lens. After correction for the dependence of the sensitivity of the detecting instruments on the polarization, the measurements gave $P(\pi/2) = 0.09 \pm 0.09$, in satisfactory agreement with the theoretical value of 0.143 obtained from Eq. (17) with $\theta = \pi/2$. The estimated uncertainty in this measurement was relatively large, chiefly because the intensity of the red satellite from the 4^1F^0 state was fainter than that from the 5^1F^0 state by about a factor of 15, and was further reduced by the insertion of the Polaroid filter, which made the measurement of its intensity more difficult. Although we did not do it, it is clear that more precise measurements of the polarization of the light emitted in two or more directions would permit spectroscopic determination of the direction of the electric field also.

V. CONCLUSIONS

The experiment shows that in certain cases spectroscopic measurements of two-quantum transitions in a plasma can provide a nonperturbing means of measuring the frequency, the intensity, and the direction of oscillating electric fields in a plasma. If the fields can be modulated, as in this experiment, to permit the use of phase-sensitive detectors, fields of the order of 50 V/cm can be studied in this way. If the fields result from natural plasma phenomena such as instabilities, waves, or plasma oscillations, this advantage is usually absent, and field strengths of the order of 1000 V/cm may be necessary before the satellites become observable above the wing of the allowed line. In either case, care in interpreting the results is necessary because of the necessity of knowing or measuring the relative populations of the two upper states of the transitions involved. Measurement of the shift of a spectral line is much easier, but yields information only about the strength of the electric

field.

ACKNOWLEDGMENTS

The authors wish to thank the other members of the Berkeley plasma physics group for many helpful discussions during the course of this work. We are especially grateful to Dr. K. Halbach and his co-workers who carried out the curve-fitting by computer, to D. B. Hopkins for help and advice in microwave technology, to W. A. Berlund who made the quartz discharge tube, and to E. B. Hewitt for his aid in operating the experiment and reducing the data.

---

*This work was done under the auspices of the U. S. Atomic Energy Commission.

†Permanent address: Institut für Plasma Physik, Garching bei München, Germany.

[1]R. Gorenflo and Y. Kovetz, Numerische Mathematik 8, 392 (1966).

[2]E. Schrödinger, Z. Physik 78, 309 (1932).

[3]D. I. Blochinzew, Phys. Z. Sowjetunion 4, 501 (1933).

[4]V. E. Mitsuk, Sov. Phys. – Tech. Phys. 3, 1223 (1958).

[5]E. V. Lifshits, A. K. Berezin, and Yu. M. Lyapkalo, Sov. Phys. – Tech. Phys. 11, 798 (1966).

[6]M. Baranger and B. Mozer, Phys. Rev. 123, 25 (1961).

[7]J. Reinheimer, J. Quant. Spectry. Radiative Transfer 4, 671 (1964).

[8]J. L. Powell and B. Crasemann, Quantum Mechanics (Addison-Wesley Publishing Co., Inc., Reading, Mass., 1961), Chap. 11.

[9]W. Heitler, The Quantum Theory of Radiation (Oxford University Press, London, 1954), 3rd Ed., Chap. V.

[10]H. A. Bethe and E. E. Salpeter, Quantum Mechanics of One- and Two-Electron Atoms (Springer-Verlag, Berlin, 1957), pp. 253 and 254.

[11]See Ref. 10, Eq. (60.8), p. 253.

[12]See Ref. 8, Eq. (11-207), p. 429.

[13]W. C. Martin, J. Res. Natl. Bur. Std. (U.S.) A64, 19 (1959).

[14]C. H. Townes and A. L. Schawlow, Microwave Spectroscopy (McGraw-Hill Book Co., New York, 1955), Chap. 10.

[15]K. Halbach, in Proceedings of the Second International Conference on Magnet Technology, Oxford University, 1967 (Rutherford High Energy Laboratory, Chilton, England, 1967), p. 47; also University of California Radiation Laboratory Report No. 17436, July 1967.

[16]See Ref. 10, Eq. (56.4), p. 242.

[17]E. L. Ginzton, Microwave Measurements (McGraw-Hill Book Co., New York, 1957), Chap. 9.

[18]J. D. Jobe and R. M. St. John, J. Opt. Soc. Am. 57, 1449 (1967).